The Plant Cell, Vol. 19: 2763–2775, September 2007, www.plantcell.org

The *Arabidopsis CLASP* Gene Encodes a Microtubule-Associated Protein Involved in Cell Expansion and Division [W]

J. Christian Ambrose, Tsubasa Shoji,[1] Amanda M. Kotzer, Jamie A. Pighin, and Geoffrey O. Wasteneys[2]

University of British Columbia, Vancouver, British Columbia, Canada

Controlling microtubule dynamics and spatial organization is a fundamental requirement of eukaryotic cell function. Members of the ORBIT/MAST/CLASP family of microtubule-associated proteins associate with the plus ends of microtubules, where they promote the addition of tubulin subunits into attached kinetochore fibers during mitosis and stabilize microtubules in the vicinity of the plasma membrane during interphase. To date, nothing is known about their function in plants. Here, we show that the *Arabidopsis thaliana* CLASP protein is a microtubule-associated protein that is involved in both cell division and cell expansion. Green fluorescent protein–CLASP localizes along the full length of microtubules and shows enrichment at growing plus ends. Our analysis suggests that CLASP promotes microtubule stability. *clasp-1* T-DNA insertion mutants are hypersensitive to microtubule-destabilizing drugs and exhibit more sparsely populated, yet well ordered, root cortical microtubule arrays. Overexpression of *CLASP* promotes microtubule bundles that are resistant to depolymerization with oryzalin. Furthermore, *clasp-1* mutants have aberrant microtubule preprophase bands, mitotic spindles, and phragmoplasts, indicating a role for At CLASP in stabilizing mitotic arrays. *clasp-1* plants are dwarf, have significantly reduced cell numbers in the root division zone, and have defects in directional cell expansion. We discuss possible mechanisms of CLASP function in higher plants.

INTRODUCTION

Microtubules are essential for eukaryotic cell division, expansion, and differentiation. In plants, the timing, placement, and orientation of these processes contributes to development by defining the axes of tissue and organ growth. Therefore, identifying the factors that regulate the diverse structural configurations that plant microtubules assume is critical for understanding plant growth and development. Because microtubule assembly in centrosome-free higher plant cells is highly dispersed, it has been suggested that self-organizational mechanisms involving microtubule-associated proteins (MAPs), which include kinesin motor proteins, take on a fundamental role in modulating higher plant microtubule function and organization (Smirnova and Bajer, 1994; Wasteneys, 2002; Dixit and Cyr, 2004a, 2004b; Ehrhardt and Shaw, 2006).

Several classes of MAPs have now been identified in plants (Sedbrook, 2004; Hamada, 2007). These proteins influence microtubule organization in a variety of ways, including modulating microtubule dynamic properties (Dhonukshe and Gadella, 2003; Perrin et al., 2007); effecting interactions between microtubules, such as cross-linking and/or sliding (Chan et al., 1999; Shaw et al., 2003; Dixit and Cyr, 2004a, 2004b; Ambrose and Cyr, 2007; Perrin et al., 2007); microtubule severing (Stoppin-Mellet et al., 2002, 2006); and γ-tubulin–dependent microtubule branching (Wasteneys and Williamson, 1989; Wasteneys, 2002; Murata et al., 2005). Some of these proteins appear to be plant-specific or at least restricted to certain taxa (Furutani et al., 2000; Buschmann et al., 2004; Nakajima et al., 2004; Sedbrook et al., 2004; Shoji et al., 2004; Perrin et al., 2007). Others are close homologs of paneukaryotic proteins, whose functions are likely to be essential and therefore highly conserved (Whittington et al., 2001; Chan et al., 2003; Van Damme et al., 2004; Ambrose et al., 2005; Dixit et al., 2006). One such highly conserved MAP is MOR1, the plant member of the XMAP215/chTOG/Dis1/MOR1 family (Gard et al., 2004). Identified in *Arabidopsis thaliana* in three independent forward genetic screens as the *mor1* (Whittington et al., 2001), *gem1* (Twell et al., 2002), and *rid5* (Konishi and Sugiyama, 2003) mutant alleles, and as MAP200 after purification from tobacco (*Nicotiana tabacum*) culture cells (Hamada et al., 2004), *MOR1* occurs as a single-copy gene (Whittington et al., 2001; Gard et al., 2004) and, in severe alleles, is homozygous-lethal (Twell et al., 2002). Consistent with the known function of the MAP215 family proteins in other kingdoms, MOR1 associates with and controls the dynamics and form of microtubule arrays at all stages of the cell cycle (Whittington et al., 2001; Twell et al., 2002; Hamada et al., 2004; Eleftheriou et al., 2005; Kawamura et al., 2006).

The ORBIT/MAST/CLASP family of MAPs (hereafter referred to as CLASP, for CLIP-Associated Protein) comprises a related but distinct group that shares structural similarity with the XMAP215/chTOG family proteins, containing an N-terminal DIS/TOG domain and numerous HEAT repeats (Inoue et al., 2000; Lemos et al., 2000). Like XMAP215/chTOG, CLASP proteins also

[1] Current address: Graduate School of Biological Sciences, Nara Institute of Science and Technology, Ikoma 630-0192, Japan.
[2] Address correspondence to geoffwas@interchange.ubc.ca.
The author responsible for distribution of materials integral to the findings presented in this article in accordance with the policy described in the Instructions for Authors (www.plantcell.org) is: Geoffrey O. Wasteneys (geoffwas@interchange.ubc.ca).
[W] Online version contains Web-only data.
www.plantcell.org/cgi/doi/10.1105/tpc.107.053777

promote microtubule stability, but they are unique for their role in the attachment of microtubule plus ends to the cell cortex and chromosomal kinetochores in animals and fungi (Maiato et al., 2005; Lansbergen et al., 2006). Owing to their enhanced binding affinity for growing microtubule plus ends, CLASPs are referred to as plus end tracking proteins, or +TIPs (Carvalho et al., 2003; Mimori-Kiyosue and Tsukita, 2003; Akhmanova and Hoogenraad, 2005). +TIPs are emerging as important elements in mediating microtubule behavior at the plus end and include a large number of MAPs from diverse structural classes. CLASPs promote the addition of tubulin subunits into attached kinetochore microtubule fibers and stabilize microtubule plus ends in the vicinity of the plasma membrane in animals (Maiato et al., 2005). Reduction or depletion of CLASP protein results in defects in the organization of both interphase and mitotic microtubule arrays, ultimately resulting in defective cell migration and failed mitosis in animal cells (Inoue et al., 2000; Lee et al., 2004; Drabek et al., 2006). In animals, CLASPs associate with several other cytoskeletal proteins, including the +TIPs EB1 and CLIP-170 (Akhmanova et al., 2001).

The *Arabidopsis* genome contains a single putative *CLASP* gene (Gardiner and Marc, 2003), which was identified in a proteomic screen for tubulin binding proteins (Chuong et al., 2004). The forward genetics screen for microtubule-defective mutants that identified the *MOR1* locus (Whittington et al., 2001) identified a second mutation, designated *mor2*, with a locus mapped to the lower arm of chromosome 2. Although mapping experiments identified the *CLASP* gene as a potential candidate for *MOR2*, our complementation and sequence analysis to date have revealed that the *mor2* mutation is not in the *CLASP* locus. Based on the fundamental role of CLASPs in other organisms, however, we sought to understand the role of CLASP in higher plants. Here, we show by reverse genetics and fluorescent fusion protein localization that At CLASP is a MAP involved in cell division and expansion.

RESULTS

CLASP Protein Structure and Gene Expression

The single ortholog of the CLASP/MAST/ORBIT family found in the *Arabidopsis* genome (At2g20190; herein named *CLASP*) is predicted to encode a protein of 1440 amino acids with an estimated molecular mass of 158 kD and a pI of 6.72. Like other members of this family, At CLASP is relatively large and contains an N-terminal TOG domain (Figure 1A, gray regions), which is named after the human Tumor-Overexpressed Gene (TOG) protein member of the MAP215/Dis1/TOG family. At CLASP shares 23% identity and 42% similarity with the human CLASP1 protein and shares similar domain organization with respect to HEAT repeats (Figure 1A, black regions). Human CLASPs also contain a C-terminal CLIP (for Cytoplasmic Linker Protein)–interacting domain (Figure 1A, stippled regions), which shares 28% identity and 52% similarity with the C-terminal region in At CLASP. Figure 1B shows a phylogenetic tree (generated by TreeView, based on ClustalW alignments) of several TOG domain–containing proteins, including the MAP215/Dis1/TOG family and the CLASP/MAST/ORBIT family proteins (circled).

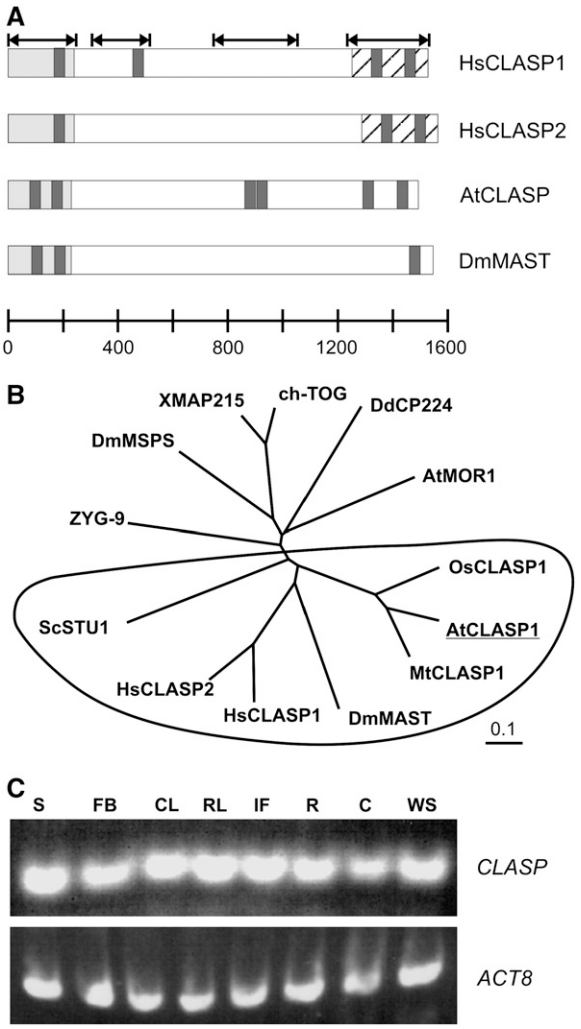

Figure 1. At CLASP Protein Domain Organization, Gene Phylogeny, and Expression.

(A) Protein domain organization of CLASP family members. HEAT repeats are black, TOG domains are gray, and CLIP-interacting domains of human orthologs are stippled. Arrows at top indicate conserved regions.

(B) Phylogenetic tree of chTOG domain proteins. Both XMAP215/MOR1 and CLASP/ORBIT/MAST (circled) families are shown.

(C) Expression of At *CLASP* as determined by RT-PCR. S, stems; FB, floral buds; CL, cauline leaves; RL, rosette leaves; IF, inflorescences; R, roots; C, cotyledons; WS, whole seedlings.

At *CLASP* contains 21 exons and 20 introns spanning a 7411-bp region and yielding a 4320-bp cDNA. To examine the expression of *CLASP*, RT-PCR was performed using gene-specific primers. As shown in Figure 1C, *CLASP* transcripts were detected in all examined tissues. This expression is consistent with database queries using Genevestigator (Zimmermann et al., 2004), which report constitutive, low-level expression of *CLASP* at all stages of development.

CLASP Associates with All Microtubule Arrays and Shows Plus End Enrichment

To determine the subcellular distribution of the CLASP protein, we engineered a reporter construct encoding the full-length *CLASP* coding sequence fused to the C terminus of green fluorescent protein (GFP) driven by the cauliflower mosaic virus 35S promoter. Stably transformed *Arabidopsis* plants and tobacco BY-2 suspension culture cell lines showing a wide range of reporter protein expression levels were selected for analysis. This fusion protein was judged to be fully functional by its ability to rescue the *clasp-1* mutant (see details below). GFP-CLASP localized to microtubules, whose identity was confirmed by their disappearance upon exposure to 20 μM oryzalin (see Supplemental Figure 1 online). Furthermore, treatment with 20 μM latrunculin B had no appreciable effect on GFP-CLASP localization, indicating that the observed localization did not represent actin microfilaments.

Plants were categorized into three groups according to GFP-CLASP fluorescence levels and distribution patterns. In low-expression (barely detectable fluorescence) plant lines, GFP-CLASP was observed solely in leaf guard cells and exhibited a modest enrichment of fluorescence (~20% higher) at the rapidly growing ends of microtubules but did not associate with microtubule ends undergoing shrinkage (Figures 2A and 2B; see also Supplemental Movie 1 and Supplemental Figure 2 online). These observations are consistent with its role as a +TIP in other organisms (Akhmanova et al., 2001; Wittmann and Waterman-Storer, 2005). At moderate expression levels, GFP-CLASP was detected in all leaf epidermal cells and distributed in a nonuniform manner along the full length of microtubules, with no apparent plus end enrichment (Figure 2C, left panel). At high expression levels, GFP-CLASP induced extensive microtubule bundling in leaf epidermal cells, as judged by the increased fluorescence intensity and thick appearance (Figure 2C, middle and right panels). Transient expression of GFP-CLASP in tobacco leaf epidermal cells also induced extensive microtubule bundling in samples showing higher levels of expression (Figure 2D).

Plants expressing GFP-CLASP were treated with the microtubule-depolymerizing drug oryzalin and visualized as above. In contrast with the rapid and complete loss of GFP-CLASP–labeled microtubule polymers in the low-expressing lines with low concentrations of oryzalin, the microtubule bundles observed with high expression resisted depolymerization, even after prolonged treatment with high concentrations of oryzalin (see Supplemental Figure 1 online).

We also examined the distribution of GFP-CLASP in dividing cells. None of the transgenic *Arabidopsis* lines expressing

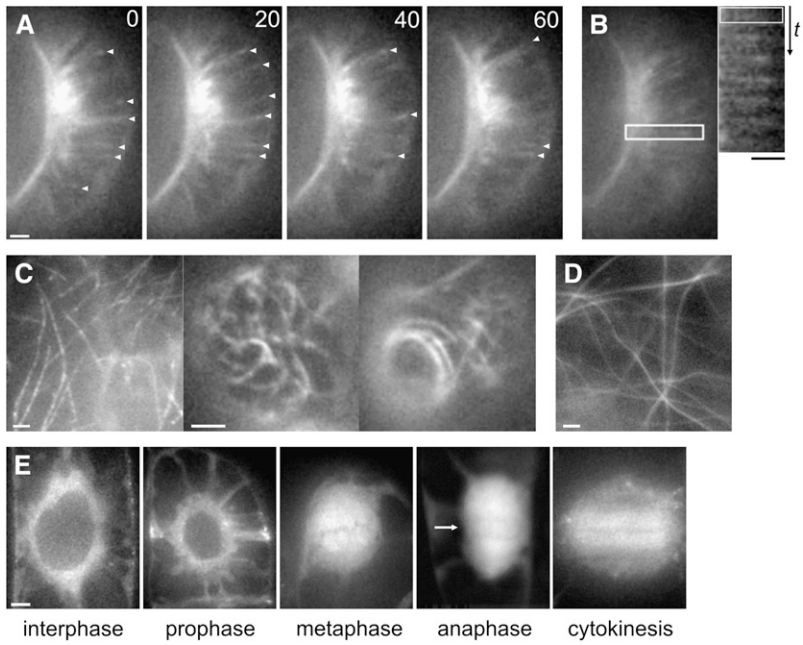

Figure 2. GFP-CLASP Is a +TIP That Localizes to All Microtubule Arrays and Induces Stable Microtubule Bundles at High Expression Levels.

(A) Stable low expression of GFP-CLASP results in microtubule labeling with enrichment at growing microtubule plus ends in leaf guard cells (arrowheads).

(B) Kymograph of the boxed region surrounding a single microtubule. The microtubule initially grows and then switches to depolymerization, at which point plus end accumulation is lost. Time is 10 s between frames.

(C) Stable moderate (left panel) and high (middle and right panels) expression of GFP-CLASP in a leaf epidermal pavement cell.

(D) Transient high expression of *35S:GFP-CLASP* in a tobacco leaf epidermal cell.

(E) Localization of GFP-CLASP to mitotic microtubule arrays when stably expressed in tobacco BY-2 cells. The arrow indicates spindle midzone accumulation during anaphase.

Bars = 5 μm.

GFP-CLASP showed detectable microtubule labeling in roots in which cell division was readily observable. This root-specific lack of fluorescence has been documented for other microtubule reporter fusions, including GFP-tubulins (Abe and Hashimoto, 2005) and GFP-EB1 (our unpublished observations), but the cause is unknown. Therefore, we examined GFP-CLASP distribution in tobacco BY-2 cells. Although a range of transgene expression levels were observed in different transformed lines, expression of GFP-CLASP was consistently low, as judged by the relatively weak fluorescence. As shown in Figure 2E, GFP-CLASP localized to all microtubule arrays in dividing cells. Although several CLASP orthologs have been detected at chromosomal kinetochores during prometaphase/metaphase, we did not observe any detectable kinetochore localization (Figure 2E, metaphase panel). Instead, GFP-CLASP localized only to spindle microtubules and the surrounding cytoplasm (Figure 2E, metaphase panel). During anaphase, fluorescence was concentrated in the spindle midzone, appearing enriched at regions of microtubule–microtubule overlap (Figure 2E, arrow). During cytokinesis, GFP-CLASP localized to microtubules of the phragmoplast (Figure 2E, cytokinesis panel). The distribution to all mitotic microtubule arrays supports a role in cell division for CLASP.

Functional Characterization of *CLASP*

In order to determine the function of CLASP in vivo, T-DNA insertional mutants were obtained from the SALK T-DNA insertion collection. Of several insertional alleles of the *CLASP* gene, we obtained two separate alleles (SALK accession numbers SALK_120061 and SALK_83034; herein termed *clasp-1* and *clasp-2*) with insertions in exon 13 and intron 11, respectively. The location of both insertions was confirmed by sequencing. Figure 3A shows the positions of these insertions in the *CLASP* gene. Because the phenotypes of *clasp-1* and *clasp-2* were indistinguishable, *clasp-1* characterization only is shown in this study. Loss of transcript was confirmed by RT-PCR with primers downstream of the T-DNA insertion site (Figure 3B). Not surprisingly, primers upstream of the insertion site amplified product in mutant lines (~50% less than in the wild type), although it is unknown whether truncated protein is encoded by these products.

Homozygous *clasp-1* mutants exhibited significant dwarfing at all stages of development compared with the wild type (Figures 3C to 3F). Stable expression of *35S:GFP-CLASP* in these lines rescued the dwarf phenotype (see Supplemental Figure 3 online), indicating the functionality of the transgene and confirming that the phenotype was due specifically to the loss of CLASP. In *clasp-1* plants, the lengths of etiolated hypocotyls were significantly reduced compared with those in the wild type (7.4 ± 1.9 mm for *clasp-1* versus 13.9 ± 1.36 mm in the wild type; $P < 0.05$ by Student's *t* test) (Figure 3D), as were leaf size and rosette diameter (Figure 3E). During flowering, inflorescence stems were much shorter than those of the wild type (Figure 3F) and *clasp-1* mutants displayed a marked reduction in seed production, as indicated by shortened siliques with fewer seeds.

Roots of *clasp-1* mutants were shorter than those in wild-type seedlings (Figures 4A and 4B). Interestingly, *clasp-1* mutants

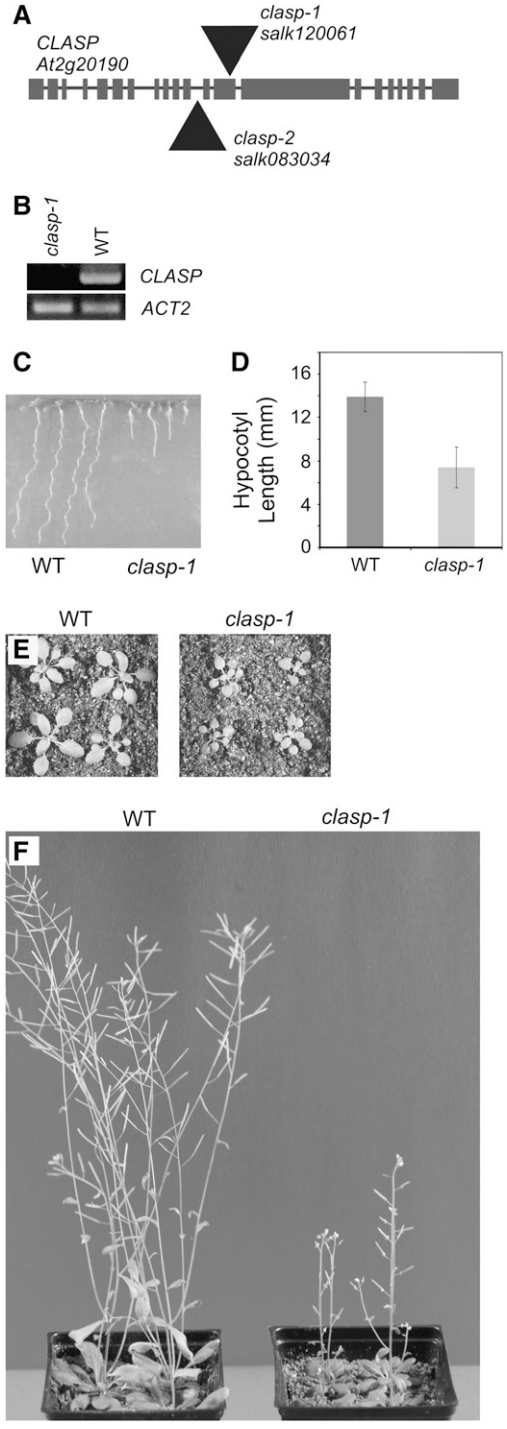

Figure 3. *clasp-1* Null Mutant Plants Exhibit Dwarfed Stature.

(A) Structure of the *CLASP* gene and positions of Salk T-DNA insertions.
(B) RT-PCR showing lack of *CLASP* transcript in 7-d-old whole seedlings of *clasp-1* mutants.
(C) Seven-day-old seedlings.
(D) Lengths of hypocotyls in 5-d-old etiolated seedlings. Error bars represent SD.
(E) Twenty-three-day-old plants.
(F) Forty-four-day-old plants.

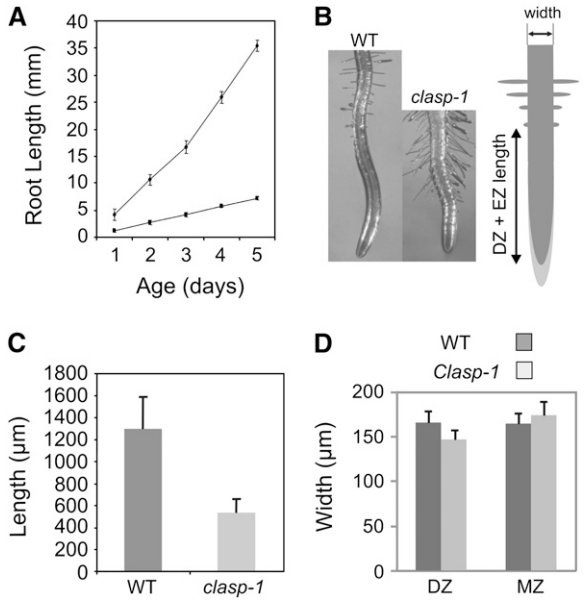

Figure 4. Root Growth Is Retarded in *clasp-1* Mutants.

(A) Lengths of primary roots in wild-type and *clasp-1* seedlings. Diamonds, wild type; squares, *clasp-1*.
(B) Images of typical wild-type and *clasp-1* roots. The graph at right illustrates the root growth parameters measured in this study. DZ, division zone; EZ, elongation zone. Width denotes mature root width.
(C) Division zone plus elongation zone lengths.
(D) Widths of roots at the division zone and mature region (MZ).
Error bars represent SD.

displayed a marked reduction in the length of the division zone and the elongation zone (Figures 4B and 4C, DZ + EZ). A small but significant reduction in elongation zone width was also observed, although this decrease was no longer apparent farther back in fully mature regions (Figure 4D, MZ). The division zones contained fewer cells compared with the wild type (Table 1), with cells beginning axial expansion at a position closer to the quiescent center. However, the proportion of mitotic cells within the division zone did not differ significantly from that in the wild type (Table 1). In the mature region of *clasp-1* roots, epidermal and cortical cells were significantly shorter than in the wild type, although, in contrast with other microtubule-related mutants, they did not appear swollen (Figure 5A, Table 1). Given the defects in the growth of *clasp-1* roots, we sought to determine cell production rates, which reflect both the number of cells in the division zone and the rates of division of cells within that zone (Rahman et al., 2007). Cell production rates were reduced by roughly half in roots of *clasp-1* (Table 1). This analysis suggests that the cells in *clasp-1* have only limited capacity for division before entering the elongation zone and that subsequent cell elongation potential is also reduced.

We also measured cell size parameters in leaves and hypocotyls (Figures 5B to 5D). Scanning electron microscopy of 7-d etiolated hypocotyls revealed that epidermal cells of *clasp-1* were shorter and wider than those of the wild type, appearing more isodiametrically shaped (Figure 5B). Similarly, leaf epidermal pavement cells were smaller and less interdigitated than wild-type cells, exhibiting a significant ($P < 0.0001$ by *t* test) reduction in mean lobe length and a corresponding increase in mean neck width (Figure 5D).

These data suggest a role for CLASP in facilitating normal cell expansion in leaves, roots, and hypocotyls, processes that are known to require microtubules. They also suggest that CLASP may be involved in determining cell numbers in organs, given that fewer cells reside in the division zone and that cell production rates are reduced in *clasp-1* roots.

Organization of Interphase Microtubule Arrays in *clasp-1* Plants

CLASP's association with microtubules and the observed cell expansion defects in the *clasp-1* mutant prompted us to examine the organization of wild-type and *clasp-1* interphase microtubules. Figure 5 shows typical antitubulin immunofluorescence patterns seen in wild-type and *clasp-1* root cells. Although whole mount immunofluorescence only labels microtubules in the root division zone and elongation zone, this facilitates comparison of the actively growing regions of the root. In agreement with the data in Figure 4 showing a reduction in the division zone and elongation zone, the region stained for microtubules in these preparations was also reduced significantly in *clasp-1* plants (Figure 6B). Interestingly, *clasp-1* roots also appeared much narrower when fixed and mounted for these preparations, but this was most likely due to a tendency of the wild-type roots to flatten after fixation. Throughout the root tip, cortical microtubules were well organized and showed a predominantly transverse orientation in *clasp-1* plants (Figure 6B). Due to the reduction in division zone size in *clasp-1* and the consequent occlusion by root cap cells, the random microtubule organization typical of recently divided G1 cells commonly seen just basal

Table 1. Root Growth and Cell Size Parameters in Wild-Type and *clasp-1* Plants

Plant	Division Zone Cell Number	Mitotic Index (%)	Cortical Cell Length (μm)	Root Growth Rate (μm/d)	Cell Production Rate (cells/d)
Wild type	40.6 ± 0.3 ($n = 16$)	3.01 ($n = 16$)	210 ± 28 ($n = 247$)	6830 ± 118 ($n = 8$)	33 ± 0.6 ($n = 8$)
clasp-1	14.6 ± 0.2 ($n = 16$)	2.47 ($n = 16$)	90 ± 18 ($n = 183$)	1350 ± 17 ($n = 10$)	15 ± 0.2 ($n = 10$)
P	5.00^{E-18}	0.45	9.00^{E-09}	2.16^{E-12}	5.95^{E-09}

Data are means ± SD. P values are from Student's *t* tests.

to the root cap was observed relatively infrequently. Instead, at the basal periphery of the root cap, *clasp-1* epidermal cells had begun directional expansion along the organ axis and contained well-ordered transverse cortical microtubules. In older, more elongated cells, cortical microtubules remained transverse in *clasp-1* as in the wild type. Despite their transverse orientation, *clasp-1* root microtubules appeared to be less abundant compared with those of the wild type, particularly in the late elongation zone (cf. insets in Figures 6A and 6B). We quantified this decreased microtubule density by measuring the distance between transversely oriented microtubules in cells of the late elongation zone (see Supplemental Figure 4 online). The mean distance between microtubules was 0.9 μm for the wild type and 1.2 μm for *clasp-1* ($n = 1439$ microtubules; $P < 10^{E-26}$ by *t* test). We also observed that, although the overall fluorescence signal in wild-type and *clasp-1* cells was similar without a postfixation detergent extraction, there was a reproducible decrease in the antitubulin fluorescence signal in *clasp-1* plants relative to the wild type when roots were detergent-extracted during processing with 0.5% Triton, which is used to increase microtubule signal to noise by removing free soluble tubulin subunits. These data indicate that the overall tubulin concentration in cells was similar but that *clasp-1* cells had a decrease in microtubule polymer levels, suggesting that microtubules are less stabilized.

To further explore the role of CLASP in microtubule stabilization, plants were grown on agar plates containing the microtubule drug oryzalin and were analyzed for root swelling at various concentrations. *clasp-1* roots began swelling with 100 nM oryzalin, compared with 300 nM for the wild type, indicating hypersensitivity to microtubule-depolymerizing drugs (Figure 7). Together, these data suggest a role for CLASP in maintaining microtubule polymer status in interphase cortical arrays and that a decrease in total tubulin polymer may affect cell expansion properties.

Organization of Mitotic Microtubule Arrays in *clasp-1* Plants

Consistent with the role that CLASP orthologs are known to play in mitosis, we observed a number of defects in microtubule organization in dividing *clasp-1* cells. As shown in Figure 8, the most obvious phenotype was seen in prophase cells, wherein a broad preprophase band (PPB) normally forms at the cortex surrounding the nucleus and gradually narrows as the cell approaches mitosis (Figures 8A and 8B). In prophase cells, 61% of *clasp-1* cells ($n = 20$) exhibited poorly developed PPBs, with nonuniform width and microtubule density, compared with 18% ($n = 33$) in the wild type (Figures 8A and 8B). Interestingly, PPB development appeared to lag behind the progression of the nuclear cycle, as 85% of *clasp-1* PPB cells ($n = 70$) contained highly condensed chromatin and lacked a nucleolus, compared with 57% in the wild type ($n = 104$). As a result, even *clasp-1* cells with very broad PPBs contained nuclei with the appearance of late prophase (Figure 8A). In addition to nonuniform and retarded PPB narrowing, 38% of PPBs in *clasp-1* ($n = 20$) formed at an angle relative to the cell axis, compared with 7% ($n = 33$) of wild-type PPBs (Figure 8B, right panel).

A number of defects were also observed in the organization of the perinuclear microtubules of prophase cells. First, whereas wild-type cells typically exhibit a robust prophase spindle that surrounds and conforms to the ellipsoid shape of the nucleus, *clasp-1* prophase spindles were often diamond-shaped, with deformations conforming to the indented surface of the accompanying nucleus (Figures 8A and 8B). Additionally, *clasp-1* cells often exhibited a difference in microtubule abundance (judged by relative fluorescence levels and intensities) between the two opposing prophase spindle poles (Figure 8B), and the position of the nuclear equator was often outside the PPB plane.

In contrast with the severe chromosome alignment defects observed with CLASP depletion in animal cells (Inoue et al.,

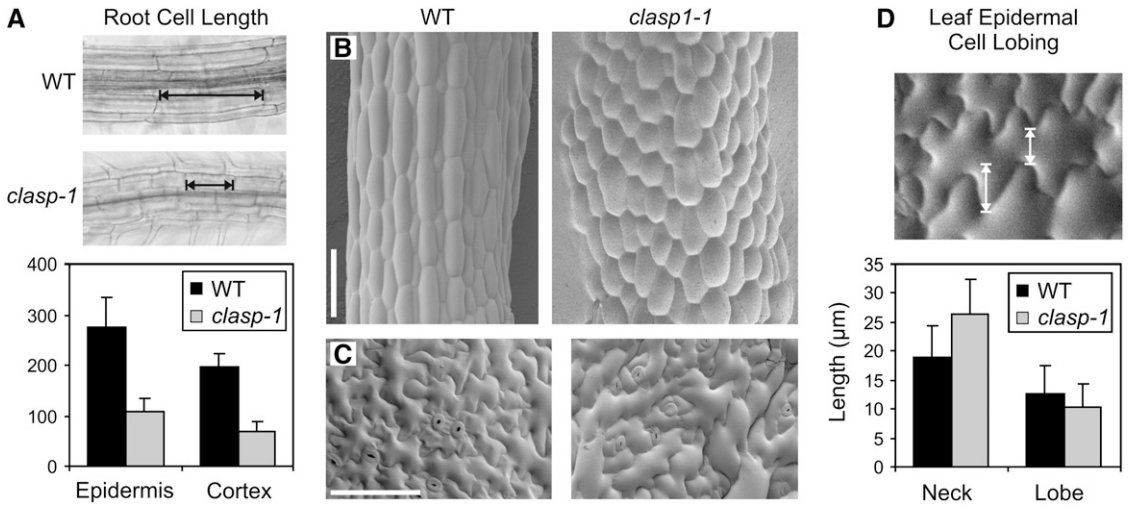

Figure 5. Cell Expansion Is Abnormal in *clasp-1* Mutants.

(A) Cell lengths in epidermal and cortical tissues of mature roots. Error bars represent SD.
(B) Scanning electron micrographs of 5-d-old etiolated hypocotyls. Bar = 100 μm.
(C) Scanning electron micrographs of 14-d-old leaf epidermal cells. Bar = 100 μm.
(D) Leaf epidermal cell lobing parameters. Arrows depict lobe length (left) and neck width (right). Error bars represent SD.

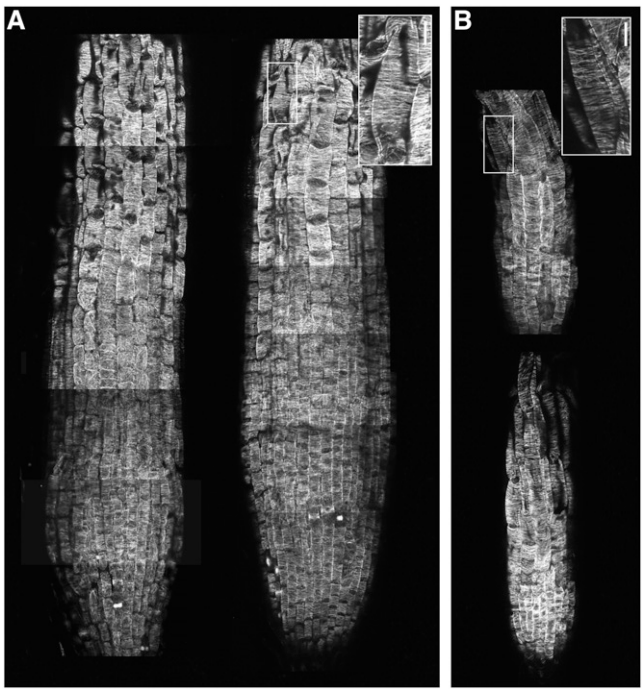

Figure 6. Microtubule Organization in Wild-Type and *clasp-1* Root Tips.

Antitubulin immunofluorescence staining of 7-d-old wild-type **(A)** and *clasp-1* **(B)** primary root tips. Images are montages of confocal micrographs representing one to three compressed Z images. Bars in insets = 10 μm.

2000; Lemos et al., 2000), chromosomes in *clasp-1* cells aligned normally and segregated with no apparent defects during metaphase and anaphase. However, *clasp-1* spindles exhibited a significant decrease in spindle length along the pole-to-pole axis, whereas the overall morphology appeared normal (Figures 8C and 8D; see Supplemental Figure 5 online). Mean metaphase spindle length was 7.3 ± 0.7 μm for the wild type and 6.1 ± 0.8 μm for *clasp-1* ($P < 10^{-6}$ by *t* test). Mean maximum anaphase spindle length was 8.0 ± 0.3 μm for the wild type and 5.71 ± 1.3 μm for *clasp-1* ($P < 0.02$ by *t* test). A decrease in mean spindle width from 5.6 ± 0.7 μm for the wild type to 4.8 ± 0.7 μm for *clasp-1* ($P < 0.004$ by *t* test) was also seen.

Similarly, during cytokinesis, a significant decrease in the length of mature phragmoplasts was observed in *clasp-1* cells (Figure 8E, bracket; see Supplemental Figure 5 online). Mean phragmoplast length was 3.8 ± 0.7 μm for the wild type and 3.1 ± 0.7 μm for *clasp-1* ($P < 10^{-10}$ by *t* test). *clasp-1* phragmoplast morphology and orientation appeared otherwise normal.

The presence of shorter spindles and phragmoplasts in *clasp-1* cells was consistent with observations in other organisms (Inoue et al., 2000; Cheeseman et al., 2005; Hannak and Heald, 2006). Together, the observations reported herein of sparse interphase cortical microtubules, malformed PPBs, and shorter spindles and phragmoplasts support a role for At CLASP in promoting microtubule polymer levels and stability.

DISCUSSION

Conserved and Divergent Functions of At CLASP

The *clasp-1* phenotype is consistent with a biochemical role for CLASP in fostering microtubule stability. The reduced cell expansion, the decrease in microtubule polymer, the enhanced oryzalin sensitivity, the impaired buildup of PPB microtubules, and the decrease in microtubule lengths in spindles and phragmoplasts are all consistent with the presence of destabilized microtubules in *clasp-1* mutants. Similarly, a role for CLASP in maintaining microtubule polymer status is demonstrated by the ability of GFP-CLASP to stabilize microtubules when expressed at high levels, leading to extensive oryzalin-resistant microtubule bundles.

Our functional analysis suggests that At CLASP has similar biochemical properties to orthologs found in other kingdoms. The reduction of microtubule polymer levels in the *clasp-1* knockout mutant is also observed after RNA interference knockdown of human CLASPs in HeLa cells (Akhmanova et al., 2001; Lee et al., 2004; Mimori-Kiyosue et al., 2005). Similarly, the highly stabilized microtubules and apparent bundling observed by overexpressing CLASP in *Arabidopsis* can also be stimulated when human CLASP is overexpressed (Akhmanova et al., 2001; Maiato et al., 2003; Lee et al., 2004; Mimori-Kiyosue et al., 2005). Transmission electron micrographs have shown microtubules tightly appressed to one another in the colcemid-resistant bundles induced by overexpressing the central microtubule binding domain of human CLASP1 (Maiato et al., 2003). This suggests that the mechanism for bundling does not rely on cross-linking by CLASP.

The cell division defects seen in *clasp-1* mutants are similar to those observed in other systems, albeit much less severe. Whereas depletion of CLASP in animals often leads to severe mitotic defects, including spindle collapse, chromosome missegregation, and failed cytokinesis, loss of *CLASP* in plant cells did not prevent chromosomes from aligning normally at the

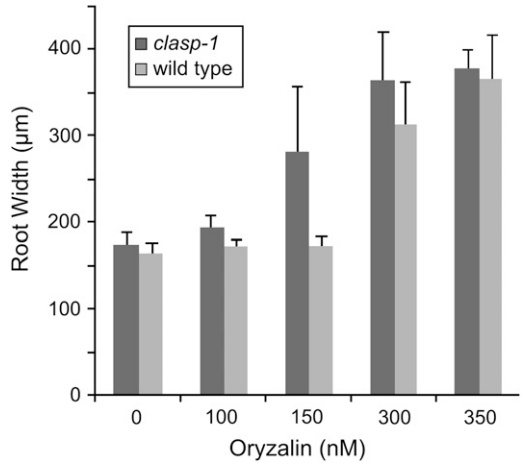

Figure 7. *clasp-1* Null Mutants Are Hypersensitive to Oryzalin.

Data are mean root widths ± SD.

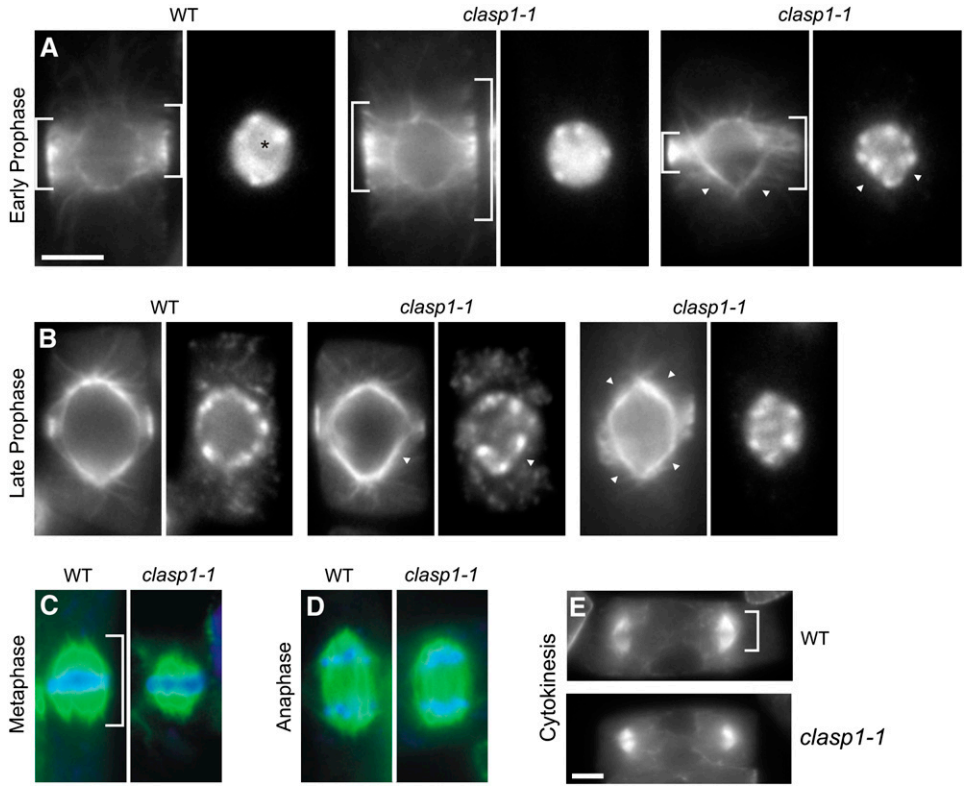

Figure 8. The Organization of Mitotic and Cytokinetic Microtubule Arrays in *clasp-1* Is Abnormal.

Antitubulin immunofluorescence staining of root squashes of 7-d-old plants is shown.
(A) Early prophase cells containing a broad PPB. The nucleolus in the wild type is indicated with an asterisk.
(B) Late prophase cells containing narrow PPBs and bipolar prophase spindles. Note the broad and disorganized *clasp-1* PPB in the right panel. This cell is beginning nuclear envelope breakdown.
(C) Metaphase spindles.
(D) Anaphase spindles.
(E) Phragmoplast during cytokinesis.
Brackets denote PPB width and spindle and phragmoplast length. Arrowheads denote indentations of the prophase spindle and nucleus. Green, microtubules, blue, 4′,6-diamidino-2-phenylindole. Bars = 5 μm.

metaphase plate and segregating to daughter cells. The major effect in dividing *clasp-1* cells observed by immunofluorescence was a decrease in spindle length and width, which has also been reported in animal cells partially depleted of CLASP (Inoue et al., 2000; Cheeseman et al., 2005; Hannak and Heald, 2006). It is unlikely that the decrease in spindle and phragmoplast size observed in *clasp-1* cells is due to the decrease in cell size, as it was recently determined that no correlation exists between cell size and the size of mitotic arrays in wild-type *Arabidopsis* root tip cells (Kawamura et al., 2006).

The relatively mild mitotic phenotype in *clasp-1* mutants, along with the lack of evidence for an association with kinetochores in our study, suggest that At CLASP is partially divergent in its mitotic function compared with its nonplant orthologs. Indeed, we would expect much more severe aberrations in the absence of CLASP if the mitotic function were identical to that in nonplant systems; in particular, lethality is frequently observed in animal cells depleted of CLASP due to the inability to complete cell division. In animal cells, CLASP is recruited to kinetochores during prometaphase, where it remains until anaphase (Maiato et al., 2003; Cheeseman et al., 2005; Hannak and Heald, 2006). It has been demonstrated that the function of CLASP at kinetochores is to foster the incorporation of tubulin subunits into attached kinetochore fibers, thereby contributing to the poleward flux of tubulin subunits (Maiato et al., 2005). Given that poleward flux is known to exist in higher plants (Dhonukshe et al., 2006), the ability of mitotic spindles to function relatively normally in the absence of At CLASP suggests a fundamentally unique flux machinery in higher plants. Identifying the components of this machinery will be of interest.

CLASP Associates with Microtubules and Shows Plus End Enrichment

Plus end–tracking proteins include a diverse array of structurally unrelated MAPs that associate with microtubule plus ends, where they appear to regulate the dynamics of microtubule plus ends and/or mediate microtubule attachment to numerous

cellular structures (Carvalho et al., 2003; Bisgrove et al., 2004; Akhmanova and Hoogenraad, 2005). In contrast with the multitude of known +TIPs in animals and fungi, only three such MAPs have been characterized to date in higher plants. They include EB1, SPR1/SKU6, and the kinesin ATK5 (Chan et al., 2003; Sedbrook et al., 2004; Ambrose et al., 2005; Dixit et al., 2006; Ambrose and Cyr, 2007). Like CLASP, SPR1/SKU6 also appears to participate in cell expansion and organ elongation, possibly via microtubule-stabilizing activity, although any function during mitosis is unknown (Nakajima et al., 2004; Sedbrook et al., 2004). ATK5 functions during mitosis to maintain mitotic spindle integrity by mediating microtubule–microtubule interactions (Ambrose et al., 2005; Ambrose and Cyr, 2007), whereas functional data for EB1 in higher plants have yet to be reported. Although some MAP215/TOG/Dis1 family MAPs behave as +TIPs (Gard et al., 2004), the plant homolog MOR1 is distributed along the full length of microtubules (Kawamura et al., 2006). Like MOR1, CLASP is involved in both cell expansion and division, but unlike MOR1, it exhibits enrichment at the plus end. Thus, its function as a plant +TIP that is involved in both cell expansion and division may be unique.

Consistent with reports from animal CLASPs and other +TIPS, we observed plus end tracking only at low transgene expression levels, while overexpression leads to enhanced microtubule lattice binding and microtubule bundling (Akhmanova et al., 2001). It is also noteworthy that the plus end enrichment observed with GFP-CLASP was relatively mild compared with that in its animal orthologs. The higher microtubule lattice association of GFP-CLASP may represent partial divergence in function or simply a difference in biochemical binding affinities. Different +TIPs associate with growing microtubule plus ends to varying extents. For example, EB1 localizes almost exclusively to the plus end when expressed at low levels (Van Damme et al., 2004; Dixit et al., 2006), whereas SPR1 and ATK5 display substantially higher microtubule lattice decoration (Sedbrook et al., 2004; Ambrose et al., 2005).

Role of CLASP in Cell Expansion

It is interesting that, despite fundamental differences in the organization of interphase microtubule arrays in plant and animal cells, in both cases the loss or depletion of CLASP leads to changes in cellular morphology. In intact plants, we observed a reduction in cell expansion in *clasp-1*, while CLASP depletion in migrating animal cells affects microtubule organization at the leading edge, which impairs cell morphology and migration (Drabek et al., 2006). In animals, these defects are due to the loss of microtubule plus end association with the plasma membrane, whereas in plants, the observed cell expansion defects may result from decreased microtubule polymer levels, which may affect cell wall properties. As with CLASP depletion in animal cells, decreased microtubule polymer in the *clasp-1* mutant may be explained by CLASP having a role in maintaining microtubule length by preventing catastrophe at the plus end.

CLASP most likely contributes to cell expansion and, in turn, organ morphology and axial extension in plants by influencing the mechanical properties of the cell wall. The requirement for microtubules in directional cell expansion is well documented, although the exact mechanisms remain unclear (Baskin, 2001; Sugimoto et al., 2003; Wasteneys, 2004; Smith and Oppenheimer, 2005). Cellulose microfibrils accumulate where cortical microtubules are most abundant (Panteris and Galatis, 2005), and according to recent studies with fluorescently labeled cellulose synthase enzymes, cellulose synthase complexes associate closely with cortical microtubules (Gardiner et al., 2003; Paredez et al., 2006). Pharmacological or genetic disruption of microtubules also impairs anisotropic cell expansion, although often this is not accompanied by any loss of parallel transverse cellulose microfibril orientation (Himmelspach et al., 2003; Sugimoto et al., 2003; Baskin et al., 2004). Like *clasp-1*, the *fra1* mutation, which targets a cortically distributed KIF4 kinesin, impairs cell growth despite having normally oriented cortical microtubules (Zhong et al., 2002). In *fra1* cells, cellulose microfibrils are variably aligned. Examining microfibril orientation in *clasp-1* mutants will be important for understanding the relationship between microtubule dynamics and cell wall mechanics.

One intriguing feature of the *clasp-1* mutants is that cortical microtubules in the root elongation zone, despite a possible reduction in polymer levels, remain well organized in transversely oriented arrays. Previous studies have demonstrated that propyzamide or oryzalin treatment, at concentrations that reduce but do not eliminate microtubules, can induce right-handed microtubule helices in root epidermal cells (Nakamura et al., 2004) or reduce microtubule density and increase randomization (Baskin et al., 2004). In one study, however, microtubule destabilization by treatment with very low levels of propyzamide promoted transverse microtubule organization in hypocotyl cells (Nakamura et al., 2004). It is possible, then, that microtubules in *clasp-1* plants are only mildly destabilized. The inhibition of axial growth but lack of dramatic organ swelling in *clasp-1* plants supports this possibility, consistent with the demonstration that root elongation inhibition occurs at lower concentrations of microtubule-destabilizing drugs than does root swelling (Collings et al., 2006).

Interestingly, *clasp-1* plants do not exhibit cell file rotation and organ twisting, phenotypes often associated with genetic or pharmacological inhibition of microtubules (Furutani et al., 2000; Abe et al., 2004; Nakamura et al., 2004; Ishida et al., 2007). Cell file rotation has been proposed to result from differential cell elongation between tissues, wherein normally elongating epidermal cells twist to accommodate the shorter cells in inner tissues (Furutani et al., 2000; Sedbrook et al., 2004; Wasteneys and Collings, 2004). It was recently shown that various mutations in either α- or β-tubulins can generate left- or right-handed helical cortical microtubule arrays in root epidermal cells (Ishida et al., 2007). Although the correlation between right-handed microtubules and left-handed twisting and vice versa is compelling, it is noteworthy that this relationship is specific to roots growing on hard agar surfaces and is not observed in *mor1-1* mutants, which display left-handed organ twisting while lacking oblique microtubule orientation (Whittington et al., 2001). In *clasp-1* plants, microtubules may not be sufficiently destabilized to induce oblique microtubule orientation and/or cell file rotation; rather, it seems more likely that the uniform reduction in cell size between layers accounts for both the reduced organ size and the lack of twisting.

Does CLASP Modulate Actin Filament Dynamics?

Perturbing the actin cytoskeleton has a profound impact on plant cell expansion properties (Bannigan and Baskin, 2005; Collings et al., 2006; Wasteneys and Collings, 2006). The recent report that human CLASPs associate directly with F-actin (Tsvetkov et al., 2007) provides insight into other potential mechanisms of At CLASP function. While we did not observe any association of GFP-CLASP with microfilaments, as demonstrated by its subcellular distribution being unaffected by actin-targeted drugs, we cannot yet rule out an interaction of CLASP with the actin cytoskeleton. It remains possible that At CLASP has an indirect association with the actin cytoskeletal network, either via adaptor proteins or via signaling mechanisms. Interestingly, CLASP orthologs in animal cells have been shown to be regulated by Rho GTPase–dependent processes (Lee et al., 2004; Wittmann and Waterman-Storer, 2005; Lansbergen et al., 2006), and in plants, Rho GTPases regulate both microtubule and actin cytoskeleton (Fu et al., 2005; Kotzer and Wasteneys, 2006). Through locally modulated activity, Rho GTPases act on both microtubules and actin filaments to effect lobe formation in leaf epidermal cells. The finding of reduced lobing in *clasp-1* leaf epidermal pavement cells suggests that At CLASP may act downstream of Rho GTPases to influence cell lobing.

Role of CLASP in PPB Function

The localization of GFP-CLASP to the PPB and the nonuniform PPB narrowing in *clasp-1* mutant cells suggests a role for CLASP in controlling PPB microtubule dynamics and organization. Low concentrations of oryzalin produce misaligned PPBs (Baskin et al., 2004), and taxol inhibits PPB narrowing, indicating the requirement of microtubule dynamics during PPB development (Panteris et al., 1995; Baluska et al., 1996). Indeed, microtubules have been demonstrated to become more dynamic in the PPBs of BY-2 cells (Dhonukshe and Gadella, 2003), although earlier studies did not detect such a change in *Tradescantia* PPBs (Hush et al., 1994). It is possible that microtubules in *clasp-1* cells are less dynamic and that the requirement for enhanced dynamics in the PPB make it more susceptible to perturbation. Alternatively, the possible interplay of CLASP with the actin cytoskeleton may also be a factor in the *clasp-1* PPB phenotype. Indeed, treatment with actin-depolymerizing drugs induces the broadening of previously narrowed PPBs, indicating a requirement of actin for proper PPB formation (Eleftheriou and Palevitz, 1992). Future studies directed at identifying CLASP's role in the regulation of microtubule dynamics will be critical for understanding the spatial organization of microtubule arrays in plant cells.

METHODS

Plant Materials and Growth Conditions

Arabidopsis thaliana seeds were cold-treated for 48 h after planting to synchronize germination. Seedlings were grown aseptically on Hoagland medium solidified with 1.2% agar at 23°C with a 16-h-light/8-h-dark cycle. Two-week-old plants were transferred to soil and further grown under the same growth conditions. The *clasp-1* mutant was backcrossed to ecotype Columbia twice prior to analysis.

Tobacco (*Nicotiana tabacum*) BY-2 cells were subcultured on a weekly basis by diluting 1:50 into fresh BY-2 medium (4.3 g/L Murashige and Skoog salts, 100 mg/L inositol, 1 mg/L thiamine, 0.2 mg/L 2,4-D, 255 mg/L KH_2PO_4, and 3% sucrose, pH 5.0).

For *Agrobacterium tumefaciens*–mediated transformation of *Arabidopsis* plants, bacteria were suspended in 5% sucrose with 0.02% Silwet-77 and sprayed onto inflorescences of 4-week-old plants. Tobacco BY-2 suspensions were transformed by mixing 10 μL of *Agrobacterium* culture (OD = 0.6) with 2 mL of 4-d BY-2 suspension cells in the presence of 2 μM acetosyringone for 4 d, followed by plating on antibiotic-containing plates.

Cloning and Genotyping

cDNA for At *CLASP* was isolated in two pieces, which were then cloned sequentially into the plasmid pVKH18:EN6mGFP (Batoko et al., 2000). The following PCR primers were used: AMK01 (5′-GCTGCTGGATCCGGTGGTATGGAGGAAGCTTTAGAAATGGCGAG-3′), AMK27 (5′-CCGGCCGAGCTCCTCTGAGCCCCGTTTAGCGGT-3′), AMK28 (5′-GCTGCTGAGCTCAGAAATGAGAGAAGTTCTCTT-3′), and AMK02 (5′-CCGGCCGAGCTCTCAGGTGTCTGCGTCGATAGGGGCACCGTTTC-3′). Genomic DNA was isolated from leaves of 7-d-old seedlings with the quick DNA preparation method (Weigel and Glazebrook, 2002). For *clasp-1* genotyping by PCR, the primers JP22 (5′-CAATGAGGCTTGATAAAGCATTC-3′) and 120053-L (5′-AAAAGTGGCCTCTGGAAATTG-3′) were used to detect the T-DNA insertion, and 120053-L and LBa1 (5′-TGGTTCACGTAGTGGCCATCG-3′) were used to detect the wild-type gene.

RT-PCR Analysis

Tissues were rapidly frozen with liquid nitrogen, and total RNA was extracted using the RNeasy plant mini kit (Qiagen). First-strand cDNAs were synthesized from total RNA with SuperScript II reverse transcriptase (Invtrogen). The cDNAs were PCR-amplified for 35 cycles with *CLASP* primers (5′-TTCAATCAAATTTTGACGGTTGTTC-3′ and 5′-TCAGGTGTCTGCGTCGATAGGGGC-3′ for downstream of the T-DNA insertion and 5′-ATGGAGGAAGCTTTAGAAATG-3′ and 5′-CTCTCCAACTCTTATGCATC-3′ for upstream of the T-DNA insertion) or *ACTIN8* primers (5′-ATTAAGGTCGTGGCA-3′ and 5′-TCCGAGTTTGAAGAGGCTAC-3′).

Bioinformatics

Alignments were performed with ClustalW (www.ebi.ac.uk/clustalw/), and trees were generated using TreeView software (taxonomy.zoology.gla.ac.uk/rod/treeview.html). Protein domains were predicted using SMART (smart.embl-heidelberg.de/) and ScanProsite (expasy.org/tools/scanprosite/).

Immunofluorescence

For root tip squashes, seedlings were fixed and processed according to Ambrose et al. (2005). For whole root immunofluorescence, roots were processed as for squashes but were not squashed. Specimens were mounted in Citifluor AF1 antifade agent.

Fluorescence and Light Microscopy

For epifluorescence and light microscopy; a Zeiss microscope (Axiovert 200M) equipped with AxioCam HRm and a Leica stereomicroscope (M216FA) equipped with DC500 were used. Typical exposure times were 1 to 2 s, using 50% lamp intensity. For time lapses, intervals are indicated in the figures. To measure root cell sizes, plants were imaged with Nomarski optics using a 20× objective.

Confocal Microscopy

Confocal imaging was performed with a 40× plan-apochromatic water-immersion objective mounted on a Zeiss LSM 510 microscope, using the 488-nm line from an argon laser. IgG:Alexa-488 fluorescence was observed using a 488-nm dichroic filter and a 505- to 545-nm emission filter. Typical scan times were 4 s, using a line averaging of two. Slice thickness was 1.5 μm.

Drug Treatments

For oryzalin treatments, seedlings were grown on medium containing oryzalin at the indicated concentrations for 5 d. Where indicated, 20 μM latrunculin B (Calbiochem) was added from a 20 mM ethanol stock solution. A stock solution of 10 mM taxol (Sigma-Aldrich) was prepared in DMSO and diluted to 20 μM in water immediately prior to experiments. Taxol treatments were at 5 μM.

Image Processing and Analysis

Image analysis was performed using ImageJ software (http://rsb.info.nih.gov/ij/). Whole root immunofluorescence montages were constructed using Corel Draw. Cell production rates were calculated from the ratio of mature cortical root cell length to root growth rate as described by Rahman et al. (2007). The division zone and elongation zone were measured as the distance from the root tip to the emergence of root hairs. The division zone was defined as the distance from the quiescent center to the first appearance of cellular elongation.

Cryoscanning Electron Microscopy

Tissues were attached to mounting plates with Tissue-Tek (Canemco Supplies) and rapidly frozen by plunging into nitrogen slush at −200°C. The plate with attached sample was then inserted into the preparation chamber of Emitech K1250 and slowly warmed to −90°C to sublime ice crystals from the specimen surface. The cryochamber temperature was adjusted to −176°C, and specimens were sputter-coated with platinum or gold for 2 min. Samples were then transferred to a cryostage at −140°C in Hitachi S4700 FESEM.

Leaf Pavement Cell Shapes

Leaf pavement cells of third true leaves from 2-week-old seedlings were observed with cryoscanning electron microscopy as described. The width of neck regions and the length of lobes were measured as shown in Figure 4. Measurements were conducted on at least 130 cells collected from five different leaves from five individual plants. For each leaf, three photographs were taken in the midregion of the leaf.

Accession Number

The Arabidopsis Genome Initiative locus identifier for *CLASP* is At2g20190.

Supplemental Data

The following materials are available in the online version of this article.

Supplemental Figure 1. Overexpression of *GFP-CLASP* Induces Stable Microtubule Bundles.

Supplemental Figure 2. Fluorescence Intensity Plot of GFP-CLASP Along Growing and Shrinking Microtubules.

Supplemental Figure 3. Molecular Complementation of *clasp-1* Plants with *35S:GFP-CLASP*.

Supplemental Figure 4. Root Cortical Microtubules Are More Sparse in *clasp-1* Compared with the Wild Type.

Supplemental Figure 5. Spindle and Phragmoplast Lengths Are Reduced in *clasp-1*.

Supplemental Movie 1. GFP-At CLASP Is a Plus End–Tracking Protein.

ACKNOWLEDGMENTS

We acknowledge the SALK Institute Genomic Analysis Laboratory and the ABRC for providing the T-DNA knockout alleles. This study was supported by the Natural Sciences and Engineering Research Council of Canada, the Canada Foundation for Innovation, the British Columbia Knowledge Development Fund, and University of British Columbia start-up funds to G.O.W. and a Postdoctoral Fellowship for Research Abroad from the Japan Society for the Promotion of Science to T.S. Confocal and scanning electron microscopy work was carried out at the University of British Columbia Bio-Imaging Facility. We thank former members of the Wasteneys laboratory, especially Tatsuya Sakai, Juliet Ward, Madeleine Rashbrooke, and Angela Whittington, whose early work on *mor2* and CLASP led to the current study.

Received June 22, 2007; revised August 16, 2007; accepted August 21, 2007; published September 14, 2007.

REFERENCES

Abe, T., and Hashimoto, T. (2005). Altered microtubule dynamics by expression of modified alpha-tubulin protein causes right-handed helical growth in transgenic Arabidopsis plants. Plant J. **43:** 191–204.

Abe, T., Thitamadee, S., and Hashimoto, T. (2004). Microtubule defects and cell morphogenesis in the lefty1lefty2 tubulin mutant of *Arabidopsis thaliana*. Plant Cell Physiol. **45:** 211–220.

Akhmanova, A., and Hoogenraad, C.C. (2005). Microtubule plus-end-tracking proteins: Mechanisms and functions. Curr. Opin. Cell Biol. **17:** 47–54.

Akhmanova, A., Hoogenraad, C.C., Drabek, K., Stepanova, T., Dortland, B., Verkerk, T., Vermeulen, W., Burgering, B.M., De Zeeuw, C.I., Grosveld, F., and Galjart, N. (2001). Clasps are CLIP-115 and -170 associating proteins involved in the regional regulation of microtubule dynamics in motile fibroblasts. Cell **104:** 923–935.

Ambrose, J.C., and Cyr, R. (2007). The kinesin ATK5 functions in early spindle assembly in Arabidopsis. Plant Cell **19:** 226–236.

Ambrose, J.C., Li, W., Marcus, A., Ma, H., and Cyr, R. (2005). A minus-end-directed kinesin with plus-end tracking protein activity is involved in spindle morphogenesis. Mol. Biol. Cell **16:** 1584–1592.

Baluska, F., Barlow, P.W., Parker, J.S., and Volkmann, D. (1996). Symmetric reorganizations of radiating microtubules around pre- and post-mitotic nuclei of dividing cells organized within intact root meristems. J. Plant Physiol. **149:** 119–128.

Bannigan, A., and Baskin, T.I. (2005). Directional cell expansion—Turning toward actin. Curr. Opin. Plant Biol. **8:** 619–624.

Baskin, T.I. (2001). On the alignment of cellulose microfibrils by cortical microtubules: A review and a model. Protoplasma **215:** 150–171.

Baskin, T.I., Beemster, G.T., Judy-March, J.E., and Marga, F. (2004). Disorganization of cortical microtubules stimulates tangential expansion and reduces the uniformity of cellulose microfibril alignment among cells in the root of Arabidopsis. Plant Physiol. **135:** 2279–2290.

Batoko, H., Zheng, H.Q., Hawes, C., and Moore, I. (2000). A rab1 GTPase is required for transport between the endoplasmic reticulum

and Golgi apparatus and for normal Golgi movement in plants. Plant Cell **12:** 2201–2218.

Bisgrove, S.R., Hable, W.E., and Kropf, D.L. (2004). +TIPs and microtubule regulation. The beginning of the plus end in plants. Plant Physiol. **136:** 3855–3863.

Buschmann, H., Fabri, C.O., Hauptmann, M., Hutzler, P., Laux, T., Lloyd, C.W., and Schaffner, A.R. (2004). Helical growth of the Arabidopsis mutant tortifolia1 reveals a plant-specific microtubule-associated protein. Curr. Biol. **14:** 1515–1521.

Carvalho, P., Tirnauer, J.S., and Pellman, D. (2003). Surfing on microtubule ends. Trends Cell Biol. **13:** 229–237.

Chan, J., Calder, G.M., Doonan, J.H., and Lloyd, C.W. (2003). EB1 reveals mobile microtubule nucleation sites in Arabidopsis. Nat. Cell Biol. **5:** 967–971.

Chan, J., Jensen, C.G., Jensen, L.C., Bush, M., and Lloyd, C.W. (1999). The 65-kDa carrot microtubule-associated protein forms regularly arranged filamentous cross-bridges between microtubules. Proc. Natl. Acad. Sci. USA **96:** 14931–14936.

Cheeseman, I.M., MacLeod, I., Yates, J.R., III, Oegema, K., and Desai, A. (2005). The CENP-F-like proteins HCP-1 and HCP-2 target CLASP to kinetochores to mediate chromosome segregation. Curr. Biol. **15:** 771–777.

Chuong, S.D., Good, A.G., Taylor, G.J., Freeman, M.C., Moorhead, G.B., and Muench, D.G. (2004). Large-scale identification of tubulin-binding proteins provides insight on subcellular trafficking, metabolic channeling, and signaling in plant cells. Mol. Cell. Proteomics **3:** 970–983.

Collings, D.A., Lill, A.W., Himmelspach, R., and Wasteneys, G.O. (2006). Hypersensitivity to cytoskeletal antagonists demonstrates microtubule-microfilament cross-talk in the control of root elongation in *Arabidopsis thaliana*. New Phytol. **170:** 275–290.

Dhonukshe, P., and Gadella, T.W.J. (2003). Alteration of microtubule dynamic instability during preprophase band formation revealed by yellow fluorescent protein-CLIP170 microtubule plus-end labeling. Plant Cell **15:** 597–611.

Dhonukshe, P., Vischer, N., and Gadella, T.W.J. (2006). Contribution of microtubule growth polarity and flux to spindle assembly and functioning in plant cells. J. Cell Sci. **119:** 3193–3205.

Dixit, R., Chang, E., and Cyr, R. (2006). Establishment of polarity during organization of the acentrosomal plant cortical microtubule array. Mol. Biol. Cell **17:** 1298–1305.

Dixit, R., and Cyr, R. (2004a). Encounters between dynamic cortical microtubules promote ordering of the cortical array through angle-dependent modifications of microtubule behavior. Plant Cell **16:** 3274–3284.

Dixit, R., and Cyr, R. (2004b). The cortical microtubule array: From dynamics to organization. Plant Cell **16:** 2546–2552.

Drabek, K., van Ham, M., Stepanova, T., Draegestein, K., van Horssen, R., Sayas, C.L., Akhmanova, A., Ten Hagen, T., Smits, R., Fodde, R., Grosveld, F., and Galjart, N. (2006). Role of CLASP2 in microtubule stabilization and the regulation of persistent motility. Curr. Biol. **16:** 2259–2264.

Ehrhardt, D.W., and Shaw, S.L. (2006). Microtubule dynamics and organization in the plant cortical array. Annu. Rev. Plant Biol. **57:** 859–875.

Eleftheriou, E.P., Baskin, T.I., and Hepler, P.K. (2005). Aberrant cell plate formation in the *Arabidopsis thaliana* microtubule organization 1 mutant. Plant Cell Physiol. **46:** 671–675.

Eleftheriou, E.P., and Palevitz, B.A. (1992). The effect of cytochalasin-D on preprophase band organization in root-tip cells of *Allium*. J. Cell Sci. **103:** 989–998.

Fu, Y., Gu, Y., Zheng, Z.L., Wasteneys, G., and Yang, Z.B. (2005). Arabidopsis interdigitating cell growth requires two antagonistic pathways with opposing action on cell morphogenesis. Cell **120:** 687–700.

Furutani, I., Watanabe, Y., Prieto, R., Masukawa, M., Suzuki, K., Naoi, K., Thitamadee, S., Shikanai, T., and Hashimoto, T. (2000). The SPIRAL genes are required for directional control of cell elongation in *Arabidopsis thaliana*. Development **127:** 4443–4453.

Gard, D.L., Becker, B.E., and Romney, S.J. (2004). MAPping the eukaryotic tree of life: Structure, function, and evolution of the MAP215/Dis1 family of microtubule-associated proteins. Int. Rev. Cytol. **239:** 179–272.

Gardiner, J., and Marc, J. (2003). Putative microtubule-associated proteins from the Arabidopsis genome. Protoplasma **222:** 61–74.

Gardiner, J.C., Taylor, N.G., and Turner, S.R. (2003). Control of cellulose synthase complex localization in developing xylem. Plant Cell **15:** 1740–1748.

Hamada, T. (2007). Microtubule-associated proteins in higher plants. J. Plant Res. **120:** 79–98.

Hamada, T., Igarashi, H., Itoh, T.J., Shimmen, T., and Sonobe, S. (2004). Characterization of a 200 kDa microtubule-associated protein of tobacco BY-2 cells, a member of the XMAP215/MOR1 family. Plant Cell Physiol. **45:** 1233–1242.

Hannak, E., and Heald, R. (2006). Xorbit/CLASP links dynamic microtubules to chromosomes in the Xenopus meiotic spindle. J. Cell Biol. **172:** 19–25.

Himmelspach, R., Williamson, R.E., and Wasteneys, G.O. (2003). Cellulose microfibril alignment recovers from DCB-induced disruption despite microtubule disorganization. Plant J. **36:** 565–575.

Hush, J.M., Wadsworth, P., Callaham, D.A., and Hepler, P.K. (1994). Quantification of microtubule dynamics in living plant cells using fluorescence redistribution after photobleaching. J. Cell Sci. **107:** 775–784.

Inoue, Y.H., do Carmo Avides, M., Shiraki, M., Deak, P., Yamaguchi, M., Nishimoto, Y., Matsukage, A., and Glover, D.M. (2000). Orbit, a novel microtubule-associated protein essential for mitosis in *Drosophila melanogaster*. J. Cell Biol. **149:** 153–166.

Ishida, T., Kaneko, Y., Iwano, M., and Hashimoto, T. (2007). Helical microtubule arrays in a collection of twisting tubulin mutants of *Arabidopsis thaliana*. Proc. Natl. Acad. Sci. USA **104:** 8544–8549.

Kawamura, E., Himmelspach, R., Rashbrooke, M.C., Whittington, A.T., Gale, K.R., Collings, D.A., and Wasteneys, G.O. (2006). MICROTUBULE ORGANIZATION 1 regulates structure and function of microtubule arrays during mitosis and cytokinesis in the Arabidopsis root. Plant Physiol. **140:** 102–114.

Konishi, M., and Sugiyama, M. (2003). Genetic analysis of adventitious root formation with a novel series of temperature-sensitive mutants of *Arabidopsis thaliana*. Development **130:** 5637–5647.

Kotzer, A.M., and Wasteneys, G.O. (2006). Mechanisms behind the puzzle: Microtubule-microfilament cross-talk in pavement cell formation. Can. J. Bot. **84:** 594–603.

Lansbergen, G., Grigoriev, I., Mimori-Kiyosue, Y., Ohtsuka, T., Higa, S., Kitajima, I., Demmers, J., Galjart, N., Houtsmuller, A.B., Grosveld, F., and Akhmanova, A. (2006). CLASPs attach microtubule plus ends to the cell cortex through a complex with LL5beta. Dev. Cell **11:** 21–32.

Lee, H., Engel, U., Rusch, J., Scherrer, S., Sheard, K., and Van Vactor, D. (2004). The microtubule plus end tracking protein Orbit/MAST/CLASP acts downstream of the tyrosine kinase Abl in mediating axon guidance. Neuron **42:** 913–926.

Lemos, C.L., Sampaio, P., Maiato, H., Costa, M., Omel'yanchuk, L.V., Liberal, V., and Sunkel, C.E. (2000). Mast, a conserved microtubule-associated protein required for bipolar mitotic spindle organization. EMBO J. **19:** 3668–3682.

Maiato, H., Fairley, E.A., Rieder, C.L., Swedlow, J.R., Sunkel, C.E., and Earnshaw, W.C. (2003). Human CLASP1 is an outer kinetochore component that regulates spindle microtubule dynamics. Cell **113:** 891–904.

Maiato, H., Khodjakov, A., and Rieder, C.L. (2005). Drosophila CLASP is required for the incorporation of microtubule subunits into fluxing kinetochore fibres. Nat. Cell Biol. **7:** 42–47.

Mimori-Kiyosue, Y., Grigoriev, I., Lansbergen, G., Sasaki, H., Matsui, C., Severin, F., Galjart, N., Grosveld, F., Vorobjev, I., Tsukita, S., and Akhmanova, A. (2005). CLASP1 and CLASP2 bind to EB1 and regulate microtubule plus-end dynamics at the cell cortex. J. Cell Biol. **168:** 141–153.

Mimori-Kiyosue, Y., and Tsukita, S. (2003). ''Search-and-capture'' of microtubules through plus-end-binding proteins (+TIPs). J. Biochem. (Tokyo) **134:** 321–326.

Murata, T., Sonobe, S., Baskin, T.I., Hyodo, S., Hasezawa, S., Nagata, T., Horio, T., and Hasebe, M. (2005). Microtubule-dependent microtubule nucleation based on recruitment of gamma-tubulin in higher plants. Nat. Cell Biol. **7:** 961–968.

Nakajima, K., Furutani, I., Tachimoto, H., Matsubara, H., and Hashimoto, T. (2004). SPIRAL1 encodes a plant-specific microtubule-localized protein required for directional control of rapidly expanding Arabidopsis cells. Plant Cell **16:** 1178–1190.

Nakamura, M., Naoi, K., Shoji, T., and Hashimoto, T. (2004). Low concentrations of propyzamide and oryzalin alter microtubule dynamics in Arabidopsis epidermal cells. Plant Cell Physiol. **45:** 1330–1334.

Panteris, E., Apostolakos, P., and Galatis, B. (1995). The effect of taxol on *Triticum* preprophase root-cells—Preprophase microtubule band organization seems to depend on new microtubule assembly. Protoplasma **186:** 72–78.

Panteris, E., and Galatis, B. (2005). The morphogenesis of lobed plant cells in the mesophyll and epidermis: Organization and distinct roles of cortical microtubules and actin filaments. New Phytol. **167:** 721–732.

Paredez, A.R., Somerville, C.R., and Ehrhardt, D.W. (2006). Visualization of cellulose synthase demonstrates functional association with microtubules. Science **312:** 1491–1495.

Perrin, R.M., Wang, Y., Yuen, C.Y., Will, J., and Masson, P.H. (2007). WVD2 is a novel microtubule-associated protein in *Arabidopsis thaliana*. Plant J. **49:** 961–971.

Rahman, A., Bannigan, A., Sulaman, W., Pechter, P., Blancaflor, E.B., and Baskin, T.I. (2007). Auxin, actin and growth of the *Arabidopsis thaliana* primary root. Plant J. **50:** 514–528.

Sedbrook, J.C. (2004). MAPs in plant cells: Delineating microtubule growth dynamics and organization. Curr. Opin. Plant Biol. **7:** 632–640.

Sedbrook, J.C., Ehrhardt, D.W., Fisher, S.E., Scheible, W.R., and Somerville, C.R. (2004). The Arabidopsis SKU6/SPIRAL1 gene encodes a plus end-localized microtubule-interacting protein involved in directional cell expansion. Plant Cell **16:** 1506–1520.

Shaw, S.L., Kamyar, R., and Ehrhardt, D.W. (2003). Sustained microtubule treadmilling in Arabidopsis cortical arrays. Science **300:** 1715–1718.

Shoji, T., Narita, N.N., Hayashi, K., Asada, J., Hamada, T., Sonobe, S., Nakajima, K., and Hashimoto, T. (2004). Plant-specific microtubule-associated protein SPIRAL2 is required for anisotropic growth in Arabidopsis. Plant Physiol. **136:** 3933–3944.

Smirnova, E.A., and Bajer, A.S. (1994). Microtubule converging centers and reorganization of the interphase cytoskeleton and the mitotic spindle in higher plant Haemanthus. Cell Motil. Cytoskeleton **27:** 219–233.

Smith, L.G., and Oppenheimer, D.G. (2005). Spatial control of cell expansion by the plant cytoskeleton. Annu. Rev. Cell Dev. Biol. **21:** 271–295.

Stoppin-Mellet, V., Gaillard, J., and Vantard, M. (2002). Functional evidence for in vitro microtubule severing by the plant katanin homologue. Biochem. J. **365:** 337–342.

Stoppin-Mellet, V., Gaillard, J., and Vantard, M. (2006). Katanin's severing activity favors bundling of cortical microtubules in plants. Plant J. **46:** 1009–1017.

Sugimoto, K., Himmelspach, R., Williamson, R.E., and Wasteneys, G.O. (2003). Mutation or drug-dependent microtubule disruption causes radial swelling without altering parallel cellulose microfibril deposition in Arabidopsis root cells. Plant Cell **15:** 1414–1429.

Tsvetkov, A.S., Samsonov, A., Akhmanova, A., Galjart, N., and Popov, S.V. (2007). Microtubule-binding proteins CLASP1 and CLASP2 interact with actin filaments. Cell Motil. Cytoskeleton **64:** 519–530.

Twell, D., Park, S.K., Hawkins, T.J., Schubert, D., Schmidt, R., Smertenko, A., and Hussey, P.J. (2002). MOR1/GEM1 has an essential role in the plant-specific cytokinetic phragmoplast. Nat. Cell Biol. **4:** 711–714.

Van Damme, D., Bouget, F.Y., Van Poucke, K., Inze, D., and Geelen, D. (2004). Molecular dissection of plant cytokinesis and phragmoplast structure: A survey of GFP-tagged proteins. Plant J. **40:** 386–398.

Wasteneys, G.O. (2002). Microtubule organization in the green kingdom: Chaos or self-order? J. Cell Sci. **115:** 1345–1354.

Wasteneys, G.O. (2004). Progress in understanding the role of microtubules in plant cells. Curr. Opin. Plant Biol. **7:** 651–660.

Wasteneys, G.O., and Collings, D.A.C. (2004). Expanding the great divide: The cytoskeleton and axial growth. In The Plant Cytoskeleton in Cell Differentiation and Development, P.J. Hussey, ed (Boca Raton, FL: Blackwell Publishing), pp. 83–115.

Wasteneys, G.O., and Collings, D.A.C. (2006). The cytoskeleton and co-ordination of directional expansion in a multicellular context. In The Expanding Cell, J.P. Verbelen and K. Vissenberg, eds (Berlin: Springer-Verlag), pp. 217–248.

Wasteneys, G.O., and Williamson, R.E. (1989). Reassembly of microtubules in *Nitella tasmanica*—Assembly of cortical microtubules in branching clusters and its relevance to steady-state microtubule assembly. J. Cell Sci. **93:** 705–714.

Weigel, D., and Glazebrook, J. (2002). Arabidopsis: A Laboratory Manual. (Cold Spring Harbor, NY: Cold Spring Harbor Laboratory Press).

Whittington, A.T., Vugrek, O., Wei, K.J., Hasenbein, N.G., Sugimoto, K., Rashbrooke, M.C., and Wasteneys, G.O. (2001). MOR1 is essential for organizing cortical microtubules in plants. Nature **411:** 610–613.

Wittmann, T., and Waterman-Storer, C.M. (2005). Spatial regulation of CLASP affinity for microtubules by Rac1 and GSK3 beta in migrating epithelial cells. J. Cell Biol. **169:** 929–939.

Zhong, R., Burk, D.H., Morrison, W.H., III, and Ye, Z.H. (2002). A kinesin-like protein is essential for oriented deposition of cellulose microfibrils and cell wall strength. Plant Cell **14:** 3101–3117.

Zimmermann, P., Hirsch-Hoffmann, M., Hennig, L., and Gruissem, W. (2004). GENEVESTIGATOR. Arabidopsis microarray database and analysis toolbox. Plant Physiol. **136:** 2621–2632.